The late to early time behaviour of an expanding plasma: hydrodynamisation from exponential asymptotics

View the article online for updates and enhancements.

You may also like

The late to early time behaviour of an expanding plasma: hydrodynamisation from exponential asymptotics

Inês Aniceto[1,*] , **Daniel Hasenbichler**[1]
and Adri Olde Daalhuis[2]

[1] School of Mathematical Sciences, University of Southampton, Southampton, United Kingdom
[2] School of Mathematics and Maxwell Institute for Mathematical Sciences, The University of Edinburgh, Edinburgh, United Kingdom

E-mail: i.aniceto@soton.ac.uk

Abstract

We use exponential asymptotics to match the late time temperature evolution of an expanding conformally invariant fluid to its early time behaviour. We show that the rich divergent transseries asymptotics at late times can be used to interpolate between the two regimes with exponential accuracy using the well-established methods of hyperasymptotics, Borel resummation and transasymptotics. This approach is generic and can be applied to any interpolation problem involving a local asymptotic transseries expansion as well as knowledge of the solution in a second region away from the expansion point. Moreover, we present *global analytical properties* of the solutions such as analytic approximations to the locations of the square-root branch points, exemplifying how the summed transseries contains within itself information about the observable in regions with different asymptotics.

Keywords: resummation, relativistic hydrodynamics,
exponential asymptotics, bjorken flow, transseries

(Some figures may appear in colour only in the online journal)

---

* Author to whom any correspondence should be addressed.

1. Introduction

Viscous relativistic hydrodynamics is a long-wavelength effective theory which has been traditionally thought to be valid only near local thermal equilibrium. Surprisingly, hydrodynamic models can be successfully applied to certain physical systems which are far from equilibrium, such as an expanding quark-gluon plasma created from heavy-ion collisions at relativistic energies [1–4]. In those cases the hydrodynamic model contains within itself emergent, non-hydrodynamic degrees of freedom which are non-perturbative in nature and decay exponentially in time toward a hydrodynamic attractor [5]. This process is known as hydrodynamisation (see e.g. [6]). These non-hydrodynamic modes play a major role during the early times of the expanding plasma, and are quite sensitive to the different initial conditions. At the hydrodynamisation time, the system is still far from equilibrium and its pressure is quite anisotropic, but nevertheless the different initial solutions all become exponentially close to each other, and the evolution of the system towards equilibrium is effectively described by viscous hydrodynamics, via the same power series expansion in small gradients valid at late times.

From the point of view of asymptotics, however, such behaviour is expected. Mathematically, the late-time attractor is described by a divergent, asymptotic perturbative series, whose resurgent properties encode all the information about the non-perturbative modes. The information about the initial conditions is instead uniquely encoded in a set of parameters determining the strength of the (exponentially small) non-hydrodynamic modes[3]. The full description of the system can then be achieved via a so-called resurgent transseries.

Thus, when solving for the time-evolution of an observable (generally determined by some ODE/PDE within the hydrodynamic model), the initial-conditions (constrained by the physics) can dramatically change the behaviour at early-times by fixing the strength of the non-hydrodynamic modes dominating this early-time regime, while at late times the non-hydrodynamic modes are exponentially suppressed and thus negligible in terms of their numerical magnitude, washing away the information on the initial conditions, with only the hydrodynamic power-law decay towards the attractor remaining.

Having access to the behaviour of our system at an initial time, as well as a description of its late-time asymptotic behaviour, one is naturally left with a few questions: how can we match the late-time behaviour to any given initial condition? Beyond a purely numerical analysis of the observable, how can we use this matching to describe the system at all times? Can we hope to describe the analytic behaviour of our observable?

The factorial divergent nature of the late-time expansions and their resurgent properties provides a path to answer these questions. Unlike many of their convergent counterparts, it is well known that these asymptotic expansions converge to their expected results quite quickly—in fact keeping just a few terms provides a very precise approximation, which can be extended far beyond the original expansion point, in our case large time (see e.g. [7]). Moreover, there are well established asymptotic summation methods, based on the underlying resurgent properties (see e.g. [8] and references therein), which provide such an approximation with exponential accuracy, thus effectively distinguishing between the exponentially close solutions at late-times [9–11]. As we will see, some of these methods even allow us to study global analytic properties of the asymptotic observable in its domain of interest, such as existence of poles or branch points [12–15]

---

[3] The number of parameters will be in one-to-one correspondence to the elementary non-hydrodynamic modes $\sigma_i \, \mathrm{e}^{-A_i w}$.

Naturally one should start with how to interpolate our late-time solution with a given initial condition. Unlike previous work discussing this matching in the context of relativistic hydrodynamics [16, 17], where the interpolation was done using a numerical least-square fit, our approach will involve various resummation methods based on the resurgent properties of the late-time solution. We will show that these resummation methods can be used to calculate the residual parameter labelling the exponentially close late-time solutions, being also highly effective at computing the solutions with exponential accuracy. Hence they are excellent approximations for most times outside of some region at very early times, where all orders of the non-hydrodynamic exponential modes are of notable size and drive the behaviour of the system.

1.1. A simple model of hydrodynamics

We will solve the interpolation problem between late and early times for an ODE describing the evolution of the effective temperature[4] of a conformal fluid in $d = 4$ dimensions undergoing a boost-invariant expansion. The model can be regarded as a toy model for the expansion of a strongly-coupled quark-gluon-plasma created after a collision of two heavy ions beams. We assume rotational and translational invariance transverse to the collision axis. Further, we assume boost invariance with respect to boosts along the collision axis (Bjorken flow, see [18]), which is a reasonable approximation at high energies in the central rapidity region. Hence all observables in our system only depend on the proper time τ of some inertial observer. The energy momentum tensor of our system is given by,

$$T^{\mu\nu} = \mathcal{E}\, u^{\mu} u^{\nu} + (g^{\mu\nu} + u^{\mu} u^{\nu}) p(\mathcal{E}) + \Pi^{\mu\nu}. \tag{1}$$

where $g^{\mu\nu} = \mathrm{diag}(-1,1,1,1)^{\mu\nu}$ is the flat Minkowski metric, $\mathcal{E}$ is the energy density in the rest frame of the fluid, $p(\mathcal{E}) = \mathcal{E}/3$ is the pressure of a perfect conformal fluid, the vector u^{μ} is the four-velocity of the fluid, and $\Pi^{\mu\nu}$ is the shear-viscosity tensor. Conservation of energy and conformal symmetry imply:

$$\nabla_{\mu} T^{\mu\nu} = 0; \qquad T^{\mu}{}_{\mu} = 0; \qquad \mathcal{E} \sim T^4. \tag{2}$$

The third equation above states that the energy density is proportional to the fourth power of temperature $T = T(\tau)$. The most straightforward approach towards solving (2) for the temperature $T(\tau)$ is to expand the shear-stress tensor $\Pi^{\mu\nu}$ from (1) by summing all the allowed derivative terms up to a given order. However, the equations one obtains are not hyperbolic, and hence the model is acausal. An alternative way of dealing with (2) is to upgrade the shear-stress tensor $\Pi^{\mu\nu}$ to an independent field satisfying a relaxation-type differential equation. This approach, called Müller-Israel-Stewart (MIS) theory, [19–22] results in a causal model and is the one we will use in this work (see [5, 23, 24]). Instead of using the variables (τ, T), where T stands for the temperature, it is more convenient to work with the variables (w, f) defined by[5]:

$$w = T\tau; \qquad f = \frac{3\tau}{2w}\frac{\mathrm{d}w}{\mathrm{d}\tau}. \tag{3}$$

---

[4] The system is not at thermal equilibrium, hence strictly speaking there is no temperature. The effective temperature is defined as the temperature of a system at thermal equilibrium with the same energy density. In the rest of this paper we will nonetheless use the term 'temperature' to refer to T.

[5] Our definition of $f(w)$ in (3) differs from the convention in [5] by $f_{\mathrm{ours}} = \frac{3}{2} f_{\mathrm{theirs}}$. We nonetheless chose this normalisation because it leads to simpler equations.
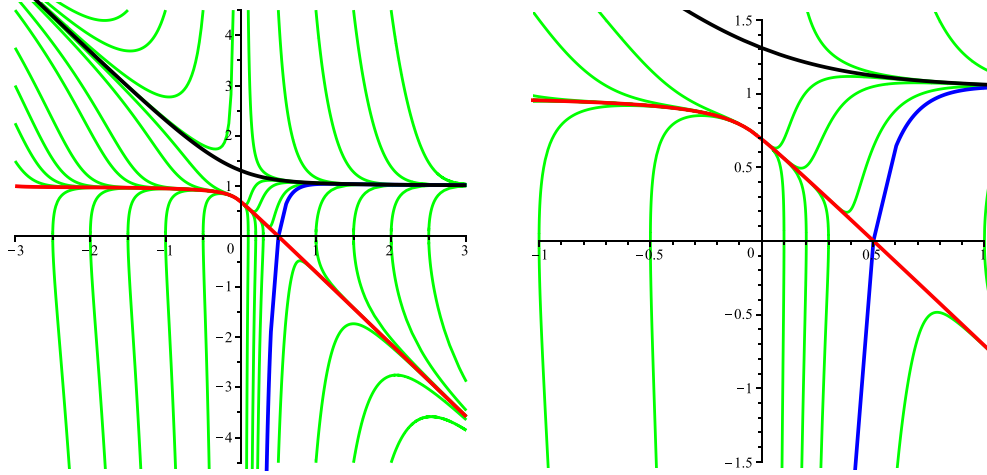
Figure 1. The real graph $(w, f(w))$ plane. The figure on the right is a zoom-in around the origin of the figure on the left. The red and blue curves are the only two solutions with a regular zero. The red curve representing $f_-(w)$ and black curve representing $f_+(w)$ are the only two solutions with finite values at the origin.

The variable w measures proper time in units of inverse temperature, and the quantity f is closely related to the pressure anisotropy[6]. The differential equation describing the evolution of $f(w)$ in MIS theory is:

$$w f(w) f'(w) + 4f(w)^2 + f(w)(-8 + Aw) + (4 - \beta - Aw) = 0. \tag{4}$$

The parameters A and β depend on phenomenological constants. If the microscopic theory behind a physical system is known, it can be used to derive these parameters. Our analysis can be performed in exactly the same way for any values of A and β. However, in this work we will use the values for A and β as in [5][7]:

$$A = \frac{3\pi}{2 - \log 2}; \qquad \beta = \frac{1}{2(2 - \log 2)}. \tag{5}$$

Let us consider the solutions of equation (4). In the solutions plot shown in figure 1 the real solutions along the real axis are displayed. There are two distinct solutions, represented by the red and black curves in figure 1, which are finite at the origin. We will call the solution represented by the black curve f_+, and the one represented by the red curve f_-. The functions f_+ and f_- are special solutions because they are attractors at $w = +\infty$, and f_+ (respectively f_-) is

---

[6] The pressure anisotropy $\mathcal{A}$ is related to f by $\mathcal{A} = 8(f - 1)$ [25].

[7] There are three phenomenological parameters defining the second-order transport coefficients which are relevant for the MIS dynamics: $C_{\tau\Pi}$, C_{λ_1} and C_η. Assuming the microscopic theory is $\mathcal{N} = 4$ SYM, these parameters have been derived using holography and are given by [26, 27]:

$$C_{\tau\Pi}^{(\text{SYM})} = \frac{2 - \log 2}{2\pi}; \quad C_{\lambda_1}^{(\text{SYM})} = \frac{1}{2\pi}; \quad C_\eta^{(\text{SYM})} = \frac{1}{4\pi}.$$

The ODE (4) is obtained by setting $C_{\lambda_1} = 0$, and identifying $A = \frac{3}{2C_{\tau\Pi}}$ and $\beta = \frac{C_\eta}{C_{\tau\Pi}}$. We followed [5] and chose $C_{\lambda_1} = 0$ because this special case leads to a very interesting mathematical structure. The other two phenomenological parameters are chosen as $C_{\tau\Pi} = C_{\tau\Pi}^{(\text{SYM})}$, $C_\eta = C_\eta^{(\text{SYM})}$, leading to (5). Note that equation (4) is only correct in the case $C_{\lambda_1} = 0$.

the attractor (respectively repellor) at $w = -\infty$. This means that all other solutions, represented by green curves in figure 1, become exponentially close to either $f_+(w)$ or $f_-(w)$ as $w \to +\infty$. An important feature of the solutions is the presence of square root branch points, whose locations we shall denote by w_s. It can be shown that equation (4) admits solutions of square root type, and admits the following analytic expansion in powers of $(w - w_s)^{1/2}$:

$$f(w) = \sum_{n=1}^{\infty} h_n(w_s) \, (w - w_s)^{n/2}, \quad \text{with } h_1^2(w_s) = \frac{2Aw_s + 2\beta - 8}{w_s}, \ h_2(w_s) = \frac{16 - 2Aw_s}{3w_s}, \ \dots.$$

(6)

The locations w_s of the branch points depend on the initial conditions we impose on $f(w)$. The presence of these square root branch points implies that the natural domain of $f(w)$ is a non-trivial Riemann surface. Note that the summation in (6) starts at $n = 1$, hence, $f(w)$ is zero at the branch points. It is easy to check that the only possible regular zero for solutions of (4) is at $w = (4 - \beta)/A \approx 0.5$, the point of intersection of red and blue curve in figure 1. Let us now analyse how the real solutions are related to each other by considering their expansions around the origin and around infinity.

1.2. Solutions around the origin

Around $w = 0$ we have the following convergent expansions:

(a) Two finite solutions at the origin:

$$f_\pm(w) = \left(1 \pm \sqrt{\beta}/2 \right) + \mathcal{O}(w), \quad w \to 0.$$

(7)

(b) A one-parameter family of solutions diverging at the origin

$$f_C(w) = Cw^{-4} + 2 + \mathcal{O}(w), \quad w \to 0.$$

(8)

We shall now analyse the solutions $f_C(w)$ and their relation to $f_+(w)$. In the solutions plot of figure 1 the green curves above the graph of $f_+(w)$ (in black) correspond to $f_C(w)$ for $C > 0$. As C becomes smaller, the green curves in figure 1 approach $f_+(w)$. In the limit $C \to 0^+, f_C(w)$ converges pointwise to $f_+(w)$ for $w \neq 0$. Hence $f_+(w)$ can be understood as the $C \to 0^+$ limit of $f_C(w)$, in which the divergence at the origin disappears. For $0 > C > C_{\text{split}} \approx -0.0874, f_C(w)$ has a square root branch point on the positive real axis. At $C = C_{\text{split}}$ this square root singularity splits into two singularities, one above and one below the real axis. The corresponding function $f_{C_{\text{split}}}(w)$ is represented by the blue curve in figure 1. For $C < C_{\text{split}}$, the function $f_C(w)$ has no square root branch points along the real axis and admits a real solution for all $w > 0$. These solutions are represented by the green curves in the bottom right corner of figure 1.

1.3. Solutions around infinity

Around $w = \infty$ we also have two distinct expansions, depending on whether the solutions converge or diverge at infinity.

(a) *Solutions of finite limit:* the solutions which converge to the hydrodynamic attractor $f_+(w)$ as $w \to +\infty$ can be described with the following transseries expansion [5]:

$$\mathcal{F}(w, \sigma) = \sum_{n=0}^{\infty} \sigma^n w^{\beta n} e^{-nAw} \Phi^{(n)}(w). \tag{9}$$

The transseries $\mathcal{F}$ describes a one-parameter family of solutions converging to the finite value $\mathcal{F} \to 1$ as $w \to +\infty$. Hence all the green curves in figure 1 which approach the black curve $f_+(w)$ have a transseries parameter σ assigned to them. The parameter σ is not determined by the equation and has to be matched with the early-time behaviour of $f(w)$ around $w = 0$, where we know all the solutions as convergent series expansions (7) and (8). We will show that the value of σ corresponding to the black and blue curves in figure 1 are approximately $\sigma_+ = -0.3493 + 0.0027i$ and $\sigma_{\text{blue}} = -14.4111 + 0.0027i$, respectively. The particular form of (9) implies that we know the amplitudes of all the non-perturbative modes once we know the transseries parameter σ. The $\Phi^{(n)}(w)$ is the divergent, asymptotic series of the nth non-perturbative sector (i.e. the nth non-hydrodynamic mode):

$$\Phi^{(n)}(w) = \sum_{k=0}^{\infty} a_k^{(n)} w^{-k}. \tag{10}$$

The coefficients $a_k^{(n)}$ above can be determined from recurrence equations obtained by using the ansatz (9) into the MIS ODE (4), and matching equal powers of σ (see appendix A). We use the convention $a_0^{(1)} = 3/2$[8]. The perturbative sector $\Phi^{(0)}(w) = 1 + \frac{\beta}{A}w^{-1} + \mathcal{O}(w^{-2})$ describes the hydrodynamic series and defines the attractor at $w \to +\infty$. Due to the factor e^{-nAw} multiplying the non-hydrodynamic series $\Phi^{(n)}(w)$, $n \geqslant 1$, the convergence of the solutions to the attractor is exponentially fast.

(b) *Growing solutions:* the solutions which are linearly growing to leading order and asymptotically approximate $f_-(w)$ as $w \to +\infty$ admit the following transseries expansion[9]

$$\Psi(p_4, w) = \sum_{k=-1}^{3} p_k w^{-k} + \sum_{k=4}^{9} w^{-k}(p_k + q_k \log w)$$
$$+ \sum_{k=10}^{14} w^{-k}(p_k + q_k \log w + r_k \log^2 w) + \dots, \tag{11}$$

with $p_{-1} = -A/5$. The first four coefficients, $n = -1, 0, 1, 2, 3, 4$, are uniquely determined by the MIS equation (4) alone. The coefficient p_4 is not determined by (4), and all other coefficients generically depend non-linearly on the coefficient p_4. Hence the transseries Ψ from (11) represents a one-parameter family of solutions. The red curve in figure 1, that is f_-, corresponds to $p_4 = -0.3474942558$. In figure 1 it can be seen that as $w \to -\infty$ the regular solutions have a transseries expansion of the form (11).

---

[8] With this convention our Stokes constant and transseries-parameter normalisation is the same as in [5, 23, 24], and choosing a different value for $a_0^{(1)}$ corresponds to a rescaling of σ.

[9] Note that the transseries Ψ from equation (11) is constructed from the basis monomials w^{-1} and $\log w$, whereas $\mathcal{F}$ is constructed from the basis monomials w^{-1} and e^{-Aw}.

The current work concerns the solutions of finite limit, also known as attractor solutions, given by the transseries (9). This transseries can be regarded as an expansion with a two-scale structure, the perturbative variable w^{-1}, as well as an exponential variable:

$$\tau \equiv \sigma w^{\beta} \mathrm{e}^{-Aw}. \tag{12}$$

In general, the transseries (9) is formally written such that the outer sum is performed over powers of τ, with coefficients $\Phi^{(n)}(w)$ depending on the variable w^{-1}. In this work we will present different summation approaches of the asymptotic functions $\Phi^{(n)}(w)$. We will also explore an alternative way of summing the transseries (9) called transasymptotic summation, in which the order of summation is reversed [13], such that the coefficients in the w^{-1}-expansion are then functions of τ (defined by a convergent Taylor series in τ). Thus the divergence of the transseries is not caused by the large-order behaviour of the exponential scales, but instead by the divergent asymptotic expansions at each order of the non-perturbative exponential. Although the transseries (9) is an expansion around $w = +\infty$, the transasymptotic approach allows us to access different regimes where τ is no longer small.

1.4. Outline

In section 2 we perform the exponentially accurate (error $\sim \mathrm{e}^{-2|Aw|}$) interpolation between late and early times with two different asymptotic methods: hyperasymptotics and Borel resummation. In particular, we show how to compute the transseries parameter σ from (9) with accuracy $\mathrm{e}^{-|Aw|}$ from the 1-parameter family of of solutions at initial time. We explain how the matching function $\sigma(C)$ can be used to illustrate the convergence of the initial solutions $f_C(w) \to f_+(w)$ as $C \to 0$ (see figure 2). This matching is performed at a chosen matching point, and the analytic continuation $f_{\mathrm{ac}}(w)$ from the origin to the matching point is performed numerically using the Taylor series method. In section 3 we introduce the transasymptotic summation and derive an asymptotic expansion for σ in closed-form at the matching point. Although the accuracy is worse with respect to hyperasymptotics and Borel resummation, it allows us to obtain analytic results which are useful far beyond the interpolation problem between late and early times and which can be employed to deduce *global* properties of the solutions. For example, one can derive an asymptotic formula for the location the of square-root branch points, and explain the differing asymptotic expansions in two different regions of our complex domain ($w \to \pm\infty$) as a direct consequence of the change in sign of the exponents $\log(\tau^n) \sim -nAw$ of our non-perturbative exponentials.

2. Interpolation between late-times and early-times

In the previous section we described the behaviour of the solutions to the MIS equation (4) both for early- and late-times. We found that there exists a one-parameter family of solutions with a finite limit at late times ($w \to +\infty$). These solutions converge exponentially fast to a hydrodynamic attractor described by a perturbative series. We saw that this series could be upgraded to the transseries (9) by including decaying exponential terms at large times. The transseries parameter σ from (9) was identified as a proxy for the amplitudes of the non-perturbative exponential modes. In the early-time regime near the origin, we found another representation of said family of solutions (8), labelled by the leading-order coefficient C of their Laurent expansion around the origin. Linking the magnitude of the non-perturbative modes of the late-time asymptotic transseries to the early-time behaviour can be very useful, and has previously

been done by numerical fitting [17, 28]. However, the fitting approach does not exploit the vast possibilities arising from the rich late time asymptotics of the solutions. In particular, the difficulty with the fitting method lies in the exponential proximity of any two distinct solutions at late times, and hence a significant deviation from the desired solution is weakly penalised at late times, while at early times the function is not accurately captured by the fit model due to the finite truncation of the transseries (9). Fortunately, given that our solution at late times is divergent asymptotic, we have a range of tools at our disposal to do the matching, whose exponential accuracy provides a way to differentiate the behaviour of the different solutions. The matching between late and early times will be achieved in three main steps:

(i) we will sum the factorial divergent expansion at late times, using exponentially accurate methods, keeping not only the perturbative series but also a non-perturbative, exponentially small part (effectively keeping the exponential accuracy). We will then evaluate this sum at a finite but large enough time w_0.

(ii) we will analytically continue the solution at the origin to the same value w_0.

(iii) the two approximations we will find depend on their respective parameters (C representing early times and σ late times) and their relation can be obtained via direct comparison.

After having found the transseries parameter for a given solution at early times, we can use the asymptotic summation methods to find exponentially accurate interpolations in the regime between early-times and late-times.

2.1. Hyperasymptotic summation

Hyperasymptotics is a resummation method which exploits the asymptotic properties of the transseries to approximate the value of a function by truncated sums [10, 11, 29, 30]. In order to compute an approximation for the solution $f(w_0)$ to the MIS ODE (4) at a finite 'matching time' w_0, we will keep terms up to linear order in the parameter σ from late time transseries solution (9). This corresponds to calculating level-one hyperasymptotics, for which we need to compute terms of the transseries sectors $\Phi^{(0)}(w)$ and $\Phi^{(1)}(w)$ from (9) (see appendix A for the computation). In level-one hyperasymptotics, the optimal number of terms N_{Hyp} at which the series expansions must be truncated is a function of the resummation point w at which we wish to resum the transseries [31]:

$$N_{\mathrm{Hyp}}(w) = 2 \left\lfloor \left| Aw \right| \right\rfloor, \tag{13}$$

where $\lfloor \cdots \rfloor$ is the floor function. Thus we need to compute the terms of the power series $\Phi^{(0)}(w)$ and $\Phi^{(1)}(w)$ to sufficiently high order (we used a maximum of 100 terms[10] for all our approximations).

The level-one hyperasymptotic summation is then given by [32][11]

$$f_{\mathrm{Hyp}}(w_0) = f_{\mathrm{Hyp},0}(w_0) + \sigma f_{\mathrm{Hyp},1}(w_0). \tag{14}$$

where the hyperasymptotic summations for the perturbative sector and the first non-perturbative sector are given by,

---

[10] Using 200 terms allows us to use the hyperasymptotic approximation with optimal precision up to $w = 7$.

[11] $f_{\mathrm{Hyp},0}(w_0)$ is not the same as the level-0 hyperasymptotics or optimal truncation, since the number of terms at which the perturbative series is truncated must be increased as more non-perturbative sectors are included in the calculation.

$$f_{\mathrm{Hyp},0}(w_0) = \sum_{m=0}^{N_{\mathrm{Hyp}}(w_0)-1} a_m^{(0)} w_0^{-m}$$

$$+ w_0^{1-N_{\mathrm{Hyp}}(w_0)} \frac{S_1}{2\pi \mathrm{i}} \sum_{m=0}^{N_{\mathrm{Hyp}}(w_0)/2-1} a_m^{(1)} F^{(1)}\left(w_0; \begin{matrix} N_{\mathrm{Hyp}}(w_0) + \beta - m \\ -A \end{matrix}\right);$$

$$f_{\mathrm{Hyp},1}(w_0) = \mathrm{e}^{-Aw_0} w_0^{\beta} \sum_{m=0}^{N_{\mathrm{Hyp}}(w_0)/2-1} a_m^{(1)} w_0^{-m}. \tag{15}$$

The function $F^{(1)}$ in (15) is called hyperterminant and defined in terms of incomplete gamma functions via [33]:

$$F^{(1)}\left(w; \begin{matrix} M \\ a \end{matrix}\right) = \mathrm{e}^{aw+i\pi M} w^{M-1} \Gamma(M)\Gamma(1-M, aw). \tag{16}$$

The quantity S_1 in (15) is the so-called Stokes constant, which may be defined as the change in the transseries parameter σ of (9) upon crossing the Stokes line, which in our case is the positive real axis. The constant S_1 has been calculated in previous work [23, 24] and is given by,

$$S_1 \approx 5.4703 \times 10^{-3}\, \mathrm{i}. \tag{17}$$

This Stokes constant can also be determined using hyperasymptotics, see appendix B, where we also provide S_1 with more precision. Note that contributions of order $\mathcal{O}\left(\sigma^2\right)$ and above in the transseries (9) are not included in level-one hyperasymptotics. The error in (15) is therefore of order $\mathrm{e}^{-2|Aw_0|}$ [31].

In order to match the late time approximation with the early time solution, we need to bring our solution at early times (equations (7) and (8)) to the finite value w_0. This is done by analytical continuation with the numerical Taylor series method (see appendix F). Let us denote the numerical approximation we obtain for $f(w_0)$ as[12]

$$f_{\mathrm{ac}}(w_0) := \mathrm{numerical\ analytic\ continuation\ of\ } f(w) \mathrm{\ from\ the\ origin,\ evaluated\ at\ the\ time\ } w_0.$$
$$\tag{18}$$

By requiring $f_{\mathrm{ac}}(w_0) = f_{\mathrm{Hyp}}(w_0)$, we obtain the following approximation for σ:

$$\sigma \approx \frac{f_{\mathrm{ac}}(w_0) - f_{\mathrm{Hyp},0}(w_0)}{f_{\mathrm{Hyp},1}(w_0)}. \tag{19}$$

By decreasing the step size and increasing the order of the Taylor expansions in the calculation of $f(w_0)$, we can achieve arbitrary accuracy, such that the error in the approximation (19) is determined by limitations of the hyperasymptotic approximation. Hence the parameter σ in (19) is accurate up to an error of order $\mathrm{e}^{-|Aw_0|}$.

Do note that the approximation for $f(w_0)$ from the late-time transseries solution can easily be extended to higher orders in the transseries parameter σ, by computing more non-hydrodynamic sectors $\Phi^{(n)}(w)$ in (9). In figure 2 the results of the early-to-late-time matching $C \leftrightarrow \sigma$ are plotted for $C > 0$. Our results are consistent with the observation in section 1 that as $(C, \sigma) \to (0^+, \sigma_+ = -0.349261 + 0.00273515\mathrm{i})$, the solutions $f_C(w)$ converge pointwise

---

[12] Note that $f_{\mathrm{ac}}(w_0)$ depends on which solution we pick around the origin from the set $\{f_+, f_-, f_C | C \in \mathbb{C}\}$.
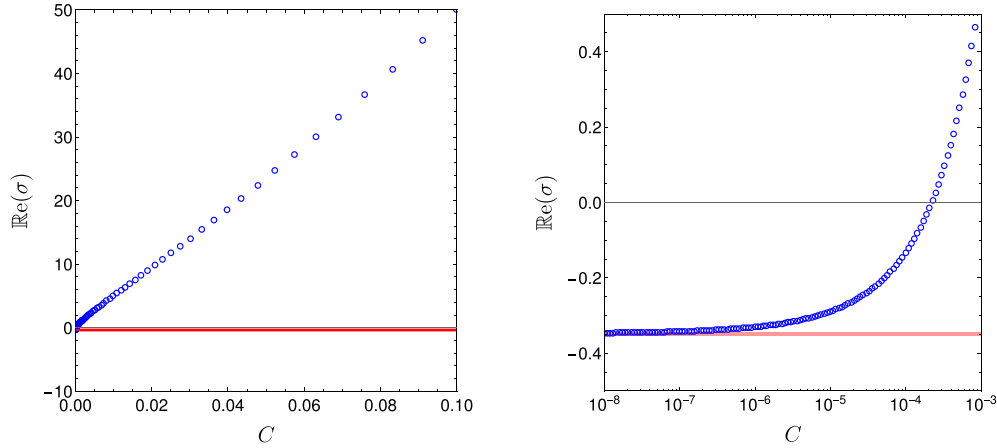
Figure 2. The real part of the matched late-time transseries parameter σ from (9) as a function of the early-time solution $f(w \sim 0)$, displayed in a linear plot (left) and a log-linear plot (right). Note that the range of values on the horizontal axis is different in each plot. The blue dots represent the matched solution $f_C(w)$ from (8) for $C > 0$, and the red line corresponds to the value $\mathbb{Re}(\sigma)$ when matched to the solution $f_+(w)$ from (7). For the imaginary part of σ we always have $\mathbb{Im}(\sigma) = \mathbb{Im}(\frac{S_1}{2})$. The convergence $\sigma(C) \to \sigma_+$ as $C \to 0$ shows the pointwise convergence $f_C(w) \to f_+(w)$.

to the solution $f_+(w)$, which is finite at the origin. The function $\sigma(C)$ in figure 2 is roughly linear (left plot) except for a tiny region around the origin $C = 0$, where the convergence towards σ_+ is very slow and is best visualised on a log-linear plot.

2.2. The Borel resummation

Another way of approximating $f(w_0)$ is through Borel resummation (see e.g. [8] for a review). The Borel transform of a series $\Phi(w) = \sum_{j \geq 0} a_j w^{-j}$ is given by[13]

$$\mathcal{B}[\Phi](\xi) = a_0 \, \delta(\xi) + \sum_{j=0}^{+\infty} \frac{a_{j+1}}{j!} \xi^j. \tag{20}$$

We truncate the series in (20) after N_0 terms[14] and calculate its Padé approximant $\mathrm{BP}_{N_0}[\Phi]$, i.e. we approximate the resulting truncated sum by a rational function $\mathrm{BP}_{N_0}[\Phi]$ with a numerator/denominator of order $\lfloor N_0/2 \rfloor$.

The Borel-Padé resummation method then consists of taking the inverse Borel transform of $\mathrm{BP}_{N_0}[\Phi]$, which is given by the Laplace transform:

$$\mathcal{S}_{N_0,\theta}\Phi(w) = a_0 + \int_0^{e^{i\theta}\infty} \mathrm{d}\xi \, e^{-w\xi} \mathrm{BP}_{N_0}[\Phi](\xi). \tag{21}$$

The resurgence properties of the transseries (9) directly translate to the existence of pole singularities of the Padé approximant $\mathrm{BP}_{N_0}[\Phi](\xi)$ in equation (21) along the positive real axis—the Stokes line—and these singularities reflect the branch cuts of the Borel transform (20),

---

[13] As usual with Borel transforms, any finite number of powers w^j, $j \geqslant 0$ need to be addressed separately, see e.g. [8].
[14] We used $N_0 = 100$, which allows us to perform the Borel resummation with optimal accuracy up to $w = 7$.

starting at all $\xi = nA$, $n \in \mathbb{N}$ (one for each exponential in the transseries). Thus we cannot resum $\mathcal{S}_{N_0,\theta}\Phi(w)$ along the positive real axis, and we need to choose integration contours that have θ slightly away from this axis, either above or below. Although this ambiguity in the choice of integration contour gives rise to an imaginary contribution for each summed sector $\mathcal{S}_{N_0,\theta}\Phi^{(n)}(w)$, there is a natural way of summing the resurgent transseries (9) such that the final result is unambiguous and real for real positive values of w—this summation procedure it the the so-called *median summation* [34, 35]. To do so we pick a small negative angle $\theta = -\varepsilon < 0$ for the integration (21), and require the imaginary value of σ in the following way (see appendix B for some more details):

$$i\,\mathbb{Im}(\sigma) = \frac{S_1}{2}. \tag{22}$$

We then obtain an approximation for $f(w_0)$ to first order in the transseries parameter σ[15], given by,

$$f_{\mathrm{B}}(w_0) \equiv \mathcal{S}_{N_0,-\varepsilon}\Phi^{(0)}(w_0) + \sigma w^\beta \, e^{-Aw_0} \mathcal{S}_{N_0,-\varepsilon}\Phi^{(1)}(w_0). \tag{23}$$

In analogy to (19), using the Borel resummation method we arrive at the following expression for σ:

$$\sigma \approx \frac{f_{\mathrm{ac}}(w_0) - \mathcal{S}_{N_0,-\varepsilon}\Phi^{(0)}(w_0)}{w^\beta \, e^{-Aw_0} \mathcal{S}_{N_0,-\varepsilon}\Phi^{(1)}(w_0)}. \tag{24}$$

Notice that for both equations (19) and (24) we only went up to linear order in σ in the approximation of $f(w_0)$. To obtain more accurate results, we could have included higher powers of σ, which amounts to including extra exponential orders[16]. For the Borel summation method we would only need to numerically compute the integrals (21) for the higher-order hydrodynamic sectors $\Phi^{(n)}(w)$ in (9), while the generalisation of the hyperasymptotic summation is a bit less straightforward. It can nonetheless be done, and we refer the reader to the literature [11, 30, 31, 36]. However, one can obtain the same accuracy if instead of increasing the number of exponentials/powers of sigma, we would just increase the value of the matching time w_0.

Once the parameter σ has been matched to a given initial condition[17], the transseries (9) can be used to find an approximation of $f(w)$ everywhere, via a summation technique such as hyerasymptotics and Borel summation described above. The hyperasymptotic method does not require computing numerical integrals, but has the disadvantage of yielding discontinuous approximations to the summed transseries: it provides a piecewise analytic approximation (which is clear from the left plot of figure 3). On the other hand, the Borel summation integrals (21) must be computed as numerical approximations at each evaluation point, but the method has the advantage of giving a continuous function of w_0.

In figure 3, we can see how different resummation methods compare with each other. In terms of accuracy the hyperasymptotic summation and the Borel resummation method are equivalent outside of a very small region near the origin, both giving an exponentially small error of approximately $e^{-2|Aw|}$ (the order of the first exponential we have neglected). We can also clearly see that the approximations given by each summation method are still accurate at very early times, even though we have only included a single exponential mode—to obtain accurate results at earlier times one would need to include further exponentials and

---

[15] We are using the transseries (9) and throwing away all the terms of order $\mathcal{O}\left(\sigma^2\right)$ and above.

[16] A similar matching was already done in [5] for the solution f_+ using Borel resummation with two exponentials.

[17] This initial condition was either the value of $f_+(0)$, or the value of C for the divergent solutions at the origin $f_C(w)$.
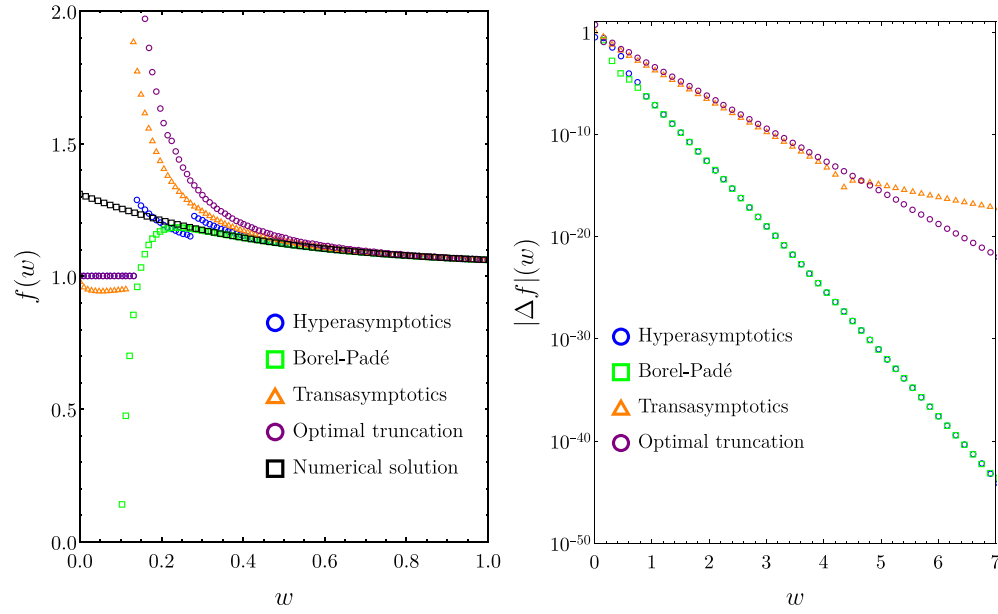
Figure 3. Left: approximations of $f(w)$ using different resummation methods for the transseries parameter $\sigma_+ = -0.3493 + 0.0027i$, corresponding to the function $f_+(w)$ (7). The numerical solution is given by the black curve on the left. Right: the absolute value of the error of the different methods, which has been computed by comparing the resummations to the numerical solution.

their respective asymptotic expansions from (9). Also in figure 3 one can find results corresponding to a transasymptotic resummation, which will be discussed in the next section 3.

Let us also briefly mention the optimal truncation method, which consists of truncating the power series of the perturbative sector before the least term[18]

$$f_{\text{opt}}(w) = \sum_{n=0}^{N_{\text{opt}}(w)-1} a_n^{(0)} w^{-n}, \quad \text{where} \quad N_{\text{opt}}(w) = \lfloor |Aw| \rfloor. \tag{25}$$

The accuracy of this optimal truncation is approximately $e^{-|Aw|}$, in agreement with the plots in figure 3.

Now that we have discussed the interpolation between late and early times using Borel resummation and hyperasymptotics, the next section will be devoted to the transasymptotic summation method.

3. Transasymptotic summation

In section 2 we saw that approximating the transseries (9) by keeping only the perturbative and the first non-perturbative sectors gives excellent approximations of exponential accuracy for the function $f(w)$ outside a small region near the origin. However, one can only truncate the transseries in this way if the exponential factors are small. Along the negative axis, the

---

[18] The formula for N_{opt} in (25) is a good approximation for the least term.

exponential monomial $\tau \sim e^{-Aw}$ defined in (12) grows arbitrarily large, and thus one cannot truncate the transseries (9) at any exponential order, since all orders of τ will contribute significantly towards the sum in that regime. This raises the question of whether the transseries can be used in regions where the exponential monomial is large enough. The answer is yes, we can exploit the fact that the divergent behaviour in the transseries comes only from large orders of the perturbative variable w^{-1}, whereas the large order behaviour of the exponential variable τ is convergent. All we need to do is change the order of summation in (9):

$$\mathcal{F}(\tau, w) = \sum_{n \geqslant 0} \sum_{r \geqslant 0} \tau^n a_r^{(n)} w^{-r} = \sum_{r \geqslant 0} \left(\sum_{n \geqslant 0} a_r^{(n)} \tau^n \right) w^{-r} \equiv \sum_{r \geqslant 0} F_r(\tau) w^{-r}. \quad (26)$$

The coefficient functions $F_r(\tau)$ are analytic at $\tau = 0$, and we will see that it is possible to systematically calculate them in closed form. This approach is called the transasymptotic summation [12, 13], and has been shown to be a powerful tool in the study of non-linear problems [14, 17, 37]. This summation procedure allows us to probe regimes where $|w| \to \infty$ but the exponentials are no longer small.

The special form of (26) allows us to compute the functions $F_r(\tau)$ by treating τ and w as independent variables. Let us start with the lowest order approximation:

$$\mathcal{F}(\tau, w) = F_0(\tau) + \mathcal{O}\left(w^{-1}\right), \quad w \to \infty. \quad (27)$$

Then F_0 obeys the ODE:

$$-1 + F_0(\tau)(1 - \tau F_0'(\tau)) = 0, \quad (28)$$

which is solved by $F_0(\tau) = 1 + W(\frac{3}{2}\tau)$[19], where W stands for the branch W_0 of the Lambert-W function (see appendix E). We can go further and calculate all $F_r(\tau)$ recursively. For $r \geqslant 1$ we find the following differential equations for F_r:

$$A\left(\tau F_0(\tau)F_r'(\tau) + (\tau F_0'(\tau) - 1)F_r(\tau)\right) = (4 - \beta)\delta_{r,1} - 8F_{r-1}(\tau) + \frac{9-r}{2}\sum_{k=0}^{r-1}F_k(\tau)F_{r-1-k}(\tau)$$

$$+ \beta\tau\sum_{k=0}^{r-1}F_k(\tau)F_{r-1-k}'(\tau) - A\tau\sum_{k=1}^{r-1}F_k(\tau)F_{r-k}'(\tau). \quad (29)$$

Note that in (29) all the derivative terms come multiplied by the variable τ, and that the variable τ does not appear other than as a multiplier of the derivatives. This motivates the convenient variable transformation $\tau \to W = W(\frac{3}{2}\tau)$. The derivatives transform as:

$$\tau\frac{d}{d\tau} = \frac{W}{1+W}\frac{d}{dW}. \quad (30)$$

With the transformation (30) it is possible to rewrite the original recursive set of ODEs (29) and integrate them exactly. The details of this calculation as well as the method of fixing the integration constants are given in appendix (C). It turns out that all the F_r are rational functions in W and can be computed exactly (see also [38, 39]). Let us now see how the functions $F_r(\tau)$ can be used to solve the interpolation problem between early and late times.

---

[19] The general solution to (28) is $F_0(\tau) = 1 + W(c\tau)$. The integration constant c is found by matching the transasymptotic expansion to the transseries (9), and depends on the choice for $a_0^{(1)}$. Our choice was $a_0^{(1)} = 3/2$.

3.1. Interpolation with transasymptotics

We want to find an approximation for the transseries parameter σ corresponding to a given solution around the origin ((8) or (7)) using the transasymptotic summation (26). The first step of our approach is the same as in section 2—using numerical analytical continuation from the origin to the matching point $w = w_0$ to obtain the numerical approximation $f_{ac}(w_0)$ (see (18)). We next compute an approximation for $\tau(w_0)$, from which the transseries parameter σ can directly be calculated using the definition of $\tau(w_0)$, equation (12). The idea is the following: we want to solve for the function $\gamma(w)$ obeying:

$$\mathcal{F}(\gamma(w), w) = \sum_{n \geqslant 0} F_r(\gamma(w)) w^{-r} = f_{ac}(w_0) = \text{constant, for } w \gg 1, \tag{31}$$

which will be equal to $\tau(w_0)$ when evaluated at the point w_0, i.e. $\gamma(w_0) = \tau(w_0)$. The function $\gamma(w)$ satisfying (31) admits a perturbative, divergent asymptotic expansion in w^{-1}:

$$\gamma(w) = \sum_{k=0}^{+\infty} \gamma_k w^{-k}, \tag{32}$$

and determining $\gamma(w)$ will correspond to finding the coefficients γ_k. Truncating the above expansion at its first term $\gamma(w) = \gamma_0 + \mathcal{O}(w^{-1})$, we find from (31) that up to leading order:

$$1 + W\left(\frac{3}{2}\gamma_0\right) = f_{an}(w_0). \tag{33}$$

Then $\gamma_0 = \tau(w_0)$ (up to leading order in w_0^{-1}), and using the definition of $\tau(w)$ (12) we finally find:

$$\sigma(w_0) = \left(f_{ac}(w_0) - 1\right) w_0^{-\beta} e^{f_{ac}(w_0) - 1 + Aw_0}\left(1 + \mathcal{O}\left(w_0^{-1}\right)\right). \tag{34}$$

This result can be easily extended to higher orders in w_0^{-1} by including higher orders in the ansatz (32) and matching powers of w^{-1} in (31). The first four coefficients of the perturbative expansion of $\gamma(w)$ are given in appendix D.

　　The transasymptotic summation (26) can also be used to re-sum the transseries by truncating the series at the term of least magnitude. The difference with respect to the classical optimal truncation is that coefficients $F_r(\tau(w))$ vary with w. The result is displayed in figure 3, where we can see that this approach slightly outperforms optimal truncation. Note that we only calculated the coefficient functions $F_r(w)$ up to $r = 15$, and so the calculation is no longer optimal after the kink in the logarithmic error plot of figure 3. Furthermore, the kink happens at a higher value of w than we would expect from the resummation point w_0 corresponding to 15 terms with classical optimal truncation given by (25).

3.2. Analytic results: branch points and global behaviour

Transasymptotics can also be used to describe *global properties* of the function $f(w)$ from (4), such as zeros, poles and branch points, or to link distinct expansions in different asymptotic regimes. This is quite remarkable given that the transasymptotic summation was derived as a *local expansion* around the point $w = +\infty$. Let us start by sketching out how the locations of the branch points may be obtained. Notice that in the solutions plot found in figure 1, the locations w_s of the square root branch points depend on the initial value problem for $f(w)$ (given by $f(0)$ for convergent solutions at the origin, or by the value of the continuous continuation of $w^4 f(w)$ at $w = 0$ for the divergent solutions). From the perspective of late-time asymptotics, this

means that the locations w_s are functions of the transseries parameter σ. As already mentioned, all the coefficient functions $F_r(\tau)$ in the transasymptotic summation (26) can be expressed as rational functions of the Lambert-W function $W(\frac{3}{2}\tau)$, which has a square-root branch point at $\tau = -\frac{2}{3}e^{-1}$. This branch point in the τ-plane translates to an infinite number of branch points in the w-plane, once we substitute $\tau = \tau(w)$ as in (12). Since the Lambert-W function appears in all the coefficient functions in the transasymptotic summation (26), we expect the function $f(w)$ to have an infinite number of square root branch points as well. The analytic information about the non-perturbative exponentials encoded in the coefficient functions $F_r(\tau)$ can be used to provide an approximation for the locations w_s.

All zeros of $f(w)$ are square root branch point singularities (see the expansions in equation (6)) with the exception of a potential regular zero at $w = (4-\beta)/A \approx 0.502$. Hence we can solve for the branch points w_s by solving the equation,

$$\mathcal{F}(w = w_s, \sigma) = 0, \tag{35}$$

for $w_s(\sigma)$, where $\mathcal{F}$ is the transasymptotic summation in equation (26). We find,

$$w_s(t) \simeq w_s^{(\text{approx})}(t) = \frac{t}{A} + \frac{\beta}{A}\log t + \frac{1}{At}\left(\beta^2 \log t + \beta^2 - 5\beta - \frac{3}{A}\right), \quad \text{as } t \to \infty, \tag{36}$$

where we have introduced the variable:

$$t \equiv t(n, \sigma) = \log\left(\frac{3\sigma e}{2A^\beta}\right) + \pi i(1 + 2n), \qquad n \in \mathbb{Z}. \tag{37}$$

The integer n in (37) parameterises the sequence of branch points. Note that (36) is the partial sum of a divergent asymptotic expansion in t, and thus equation (36) is only a good approximation for the branch points/zeros of $f(w)$ when $|t|$ is large enough. In particular, $w^{(\text{approx})}(t)$ becomes more accurate for large values of the discrete parameter n, because the auxiliary variable t grows as an affine function of n. Since the leading order approximation $w^{(\text{approx})}(t)$ from equation (36) grows linearly in t, the branch points which lie far from the origin are the ones best approximated by $w^{(\text{approx})}(t)$.

Numerically, we can compute the zeros of $f(w)$ by initially guessing the position of the branch point using (36)[20] and then using a contour integral to find an approximation for the exact location. We start by choosing a value for the transseries parameter σ and use the hyper-asymptotic approximation equation (15) to find $f(w_0)$ (at e.g. $w_0 = 10$). We then analytically continue $f(w)$ from w_0 to a point in the vicinity of our prediction (36) using the Taylor series method, $w_1 = w_s^{(\text{approx})}(t) + \varepsilon$ (e.g. $\varepsilon = 0.3$). Next we analytically continue again to compute the data on the circle $|w - w_s^{(\text{approx})}(t)| = \varepsilon$. Using the trapezoidal rule [40] we evaluate the contour integral of $\frac{wf'(w)}{f(w)}$ to obtain the zeros of $f(w)$[21]. The approximate locations obtained with equation (36) as well as the numerical results are listed in table 1, and plotted in figure 4.

There is yet another powerful application of transasymptotics, which is that it can be used to correctly predict the different asymptotic behaviour of our solutions in separate regions of the w-plane. Consider the attractor f_+ in the solutions plot of figure 1 (the black curve). At large, positive w, $f_+(w)$ converges to a finite value, while at large, negative w the same solution grows linearly with w. Therefore we have have two different asymptotic expansions, the transseries (9) at large positive w and the linearly growing expansion (11) at large negative w (which is also a transseries, but with $\log w$-monomials instead of exponentials e^{-Aw}, see [41]).

---

[20] We could also have used Padé approximants for the initial guess.

[21] Due to the square root singularity (see (36)), the branch point must be encircled twice.

Table 1. Approximations for the locations of the square-root branch points of (36) versus their numerically computed values for $\sigma = \frac{2}{3}$.

	Approx. (36)	Numerical
$n = 0$	$0.0975 + 0.6040i$	$0.1147 + 0.5076i$
$n = 1$	$0.1555 + 1.416i$	$0.1580 + 1.384i$
$n = 2$	$0.1817 + 2.276i$	$0.1827 + 2.257i$
$n = 3$	$0.1991 + 3.143i$	$0.1997 + 3.129i$
$n = 4$	$0.2122 + 4.012i$	$0.2125 + 4.001i$
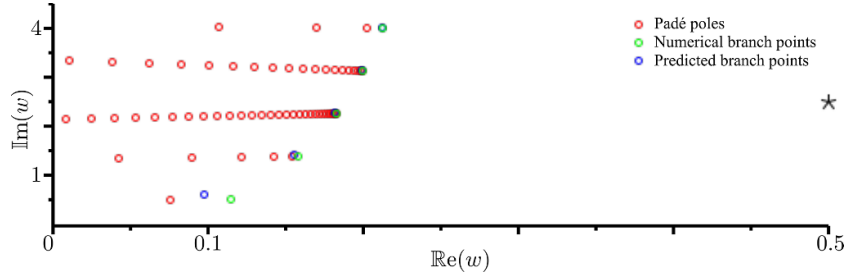
Figure 4. Branch cuts of the $f(w)$ for the case $\sigma = \frac{2}{3}$. Green dots: numerically computed branch-points. Blue dots: approximations (36) to the locations of the branch points obtained from the transasymptotic summation of the late time solution $\mathcal{F}(w)$ (9) (compare table 1). Red dots: poles for the Padé approximant (about $w = \frac{1}{2} + \frac{5}{2}i$, shown as $\star$) representing the branch cuts of the solution.

This is not surprising given the presence of square root branch points in the domain of our solutions. But it also raises an interesting question: can we somehow relate the two expansions to one another? The answer is yes, the great power of the transasymptotic approach lies in the possibility of analytically accessing regions in which the non-perturbative exponentials are no longer small. While the large, positive w limit corresponds to exponentially small values of $\tau \sim e^{-Aw}$, the large, negative w limit is associated with exponentially large values of τ. Thus when one flips the sign $w \to -w$, the powers of w^{-1} in the transasymptotic summation (26) do not change size, while the exponential variable $\tau \sim e^{-Aw}$ becomes exponentially large instead of exponentially small. Since the coefficient functions in the transasymptotic summation are just rational functions of $W(\tau)$, and the large τ expansion of $W(\tau)$ is known (see [42] and appendix E), we were able to use transasymptotics to correctly derive the first four terms of the linearly growing expansion (11). The details of the calculations in this section are beyond the scope of this publication and will be explored in an upcoming paper [43].

4. Summary/Discussion

This work focuses on solving the problem of late-time to early-time matching for arbitrary solutions of the ODE (4). We find a one-parameter family of solutions in two different regions of our domain, both at early and late time. At late times, the ODE (4) admits formal, asymptotic transseries solutions consisting of a hydrodynamic perturbative sector as well as non-hydrodynamic sectors weighed by positive integer powers of the non-perturbative exponentials e^{-Aw} (with variable w representing time). In the early time regime $w \sim 0$ there is also a one-parameter family of divergent solutions which behave asymptotically as $\sim w^{-4}$, as well

as two finite solutions which are special limits of the one-parameter family (see solution plots in figure 1). The exponentially small contributions appearing at late times can be expected to be the leading contributions at early times. Beyond the MIS case, one expects to find similar transseries solutions in other hydrodynamic systems which observe a factorially divergent late time behaviour (see e.g. [44])

The results obtained in the previous Sections were based on the well-established resummation methods of hyperasymptotics, Borel-summation and transasymptotics. Nevertheless, previous work did not exploit their strengths to do the parameter-matching and relied instead on less accurate procedures such as numerical least square fits [17, 28]. We carried out an analysis of said methods, and have shown that they are very effective tools for the parameter-matching. In terms of accuracy, the hyperasymptotic approach and the Borel resummation perform best. Both give an exponentially small error $\sim e^{-2|Aw|}$.

The hyperasymptotic approximation has discontinuities since the number of terms which are included in the series varies with w, but requires no intricate numerical computations other than determining the series coefficients of the perturbative and first non-perturbative sectors. On the other hand, the Borel resummation is a continuous function of w. However, the calculation of the Laplace transform (21) in going from the Borel-plane to the complex w-plane requires the numerical computation of an integral. As a consequence, Borel resummation is more computationally expensive than the hyperasymptotic summation, especially since said integral must be computed to exponential accuracy e^{-Aw} for the method to perform as well as the level-1 hyperasymptotic summation.

The summation methods can be made arbitrarily accurate by increasing the number of non-perturbative modes included in the approximation, as both resummation methods can be extended to include an arbitrary number of exponentials. But while the extension of Borel-summation methods to include higher exponentials is straightforward, the generalisation of hyperasymptotics beyond level-1 quickly becomes impractical.

The transasymptotic summation was originally used very effectively in the analysis of solutions of non-linear ODEs [13]. While the transasymptotic summation is less accurate in performing the interpolation, giving an error of $\sim e^{-|Aw|}$ (as opposed to $e^{-2|Aw|}$ for the methods mentioned above), it is an extremely useful tool in the study of the *global* analytic properties of the solutions. The power of the transasymptotic approach lies in encoding the behaviour of the non-perturbative exponentials in analytic closed-form expressions, which provide analytic continuations beyond the validity of the original transseries expansion. We have provided a systematic way of calculating these functions and used them to derive general analytic results such as analytic approximations to the locations of the square-root branch points as well as a way of linking distinct asymptotic expansions in two different regions of the w-plane. The preliminary results presented in this work will be studied in depth in [43].

The matching procedure we used is quite general and can be used beyond relativistic hydrodynamics. In fact, one can apply it to any interpolation problem between two different regions (e.g. late-time to early-time, strong/weak coupling, large charge to small charge), where the solutions in one region are described by resurgent, asymptotic perturbative expansions, and where the behaviour in the other regime is known analytically (e.g. [17, 45–50]).

Data availability statement

The data that support the findings of this study are available upon reasonable request from the authors.

Acknowledgment

Appendix A. Recurrence relations for $\Phi^{(1)}$ and $\Phi^{(2)}$

The recurrence relations for the coefficients of the perturbative and the first non-perturbative sector can be derived by substituting the expression,

$$f(w) = \Phi^{(0)}(w) + \sigma w^\beta e^{-Aw} \Phi^{(1)}(w), \tag{38}$$

into the MIS ODE (4). At order $\mathcal{O}(\sigma^0)$ we obtain the same ODE, but for $\Phi^{(0)}$ instead of *f*. At order $\mathcal{O}(\sigma^1)$ we find the equation,

$$\Phi^{(1)}(w)\left(-8 + Aw + (8 - Aw + \beta)\Phi^{(0)}(w) + w\partial_w \Phi^{(0)}(w)\right) + w\Phi^{(0)}(w)\partial_w \Phi^{(1)}(w) = 0. \tag{39}$$

With the series ansatz,

$$\Phi^{(n)}(w) = \sum_{j=0}^{\infty} a_j^{(n)} w^{-j}, \tag{40}$$

we obtain the recurrence relations for $\Phi^{(0)}$ and $\Phi^{(1)}$:

$$
\begin{aligned}
&a_0^{(0)} = 1; \quad a_1^{(0)} = \frac{\beta}{A}; \\
&a_j^{(0)} = \frac{1}{A}\left[8a_{j-1}^{(0)} + \frac{j-9}{2}\sum_{\ell=0}^{j-1} a_\ell^{(0)} a_{j-1-\ell}^{(0)}\right], \quad \text{for } j \geqslant 2; \\
&a_0^{(1)} \equiv \frac{3}{2}; \\
&a_j^{(1)} = \frac{1}{j}\left[(8 + \beta - j)\sum_{\ell=0}^{j-1} a_\ell^{(1)} a_{j-\ell}^{(0)} - A\sum_{\ell=0}^{j-1} a_\ell^{(1)} a_{j+1-\ell}^{(0)}\right], \quad \text{for } j \geqslant 1.
\end{aligned}
\tag{41}
$$

The coefficient $a_0^{(1)}$ is undetermined by (39), and any redefinition of $a_0^{(1)}$ can be absorbed into the transseries parameter σ.

Appendix B. The Stokes constant S_1 and median summation

An approximation for S_1 relying on hyperasymptotics is given by [51]:

$$S_1 \approx 2\pi \, \mathrm{i} \, a_{N_0}^{(0)} \left(\sum_{m=0}^{\lfloor N_0/2 \rfloor - 1} \frac{a_m^{(1)} \Gamma(N_0 + \beta - m)}{A^{N_0 + \beta - m}} \right)^{-1} \tag{42}$$

$$\approx 0.0054702985252105887650131350053326816463990385103064244677326162\mathrm{i}.$$

We did compute S_1 with (42) with an accuracy of $\mathcal{O}\left(10^{-65}\right)$ using $N_0 = 200$. Equation (42) requires knowledge of the coefficients of both the perturbative and the first non-perturbative sector. Note that it is possible to compute S_1 without knowing the coefficients of the first non-perturbative sector using the so-called large-order relations:

$$a_n^{(0)} \sim \frac{\Gamma(n + \beta)}{A^{n+\beta}} S_1 \left(a_0^{(1)} + \mathcal{O}\left(n^{-1}\right) \right), \text{as} \quad n \to \infty. \tag{43}$$

The leading order behaviour in (43) provides a sequence which converges to S_1 as $\mathcal{O}\left(n^{-1}\right)$ and involves only the free coefficient $a_0^{(1)}$ from the first non-perturbative sector, which *defines* the Stokes constant. The value in equation (42) corresponds to the choice $a_0^{(1)} = 3/2$, which we did so value of the Stokes constant is the same as in [5, 23, 24]. There is a connection between the value of the Stokes constant and the ambiguity in the value of the parameter σ. The positive real axis is a Stokes line, meaning that the Borel transform $\mathcal{B}\left[\Phi\right](\xi)$ has branch-cut singularities at the locations $\xi = A, 2A, 3A \dots$. Therefore the definition (21) is ambiguous in the choice of angle θ.

When we move the integration path across the Stokes line from below and thus increase the angle θ in (21) from $\theta_- = -\varepsilon$ to $\theta_+ = +\varepsilon$ we obtain a discontinuity in the result of the Borel resummation (21). Crossing the Stokes line in (21) while keeping the value of the transseries parameter σ from (9) constant corresponds to moving from one Riemann sheet to the other. Alternatively, we can alter the value of the transseries parameter as $\sigma \to \sigma - S_1$ in order to cancel the discontinuity. We require the result of the resummation for the whole transseries (9) to be real-valued on the positive real axis, which is known as median-resummation. The reality constraint fixes the imaginary part of the transseries parameter σ. Median resummation requires[22]

$$\mathrm{i}\,\mathbb{Im}(\sigma) = \pm \frac{S_1}{2}, \quad \text{for} \mp \theta > 0. \tag{44}$$

If we choose a convention on the path along which we carry out the integration in (21) (below/above the real axis in the Borel plane), the only degree of freedom that is left is the real part of the parameter σ, which makes sense given that we have a one-parameter family of real solutions.

Appendix C. Coefficient functions $F_r(W)$

The ODEs (29) can be rewritten as

$$\mathcal{L} F_r(W) = g_r(W); \qquad \mathcal{L} \equiv (1 + W) W \frac{\mathrm{d}}{\mathrm{d}W} - 1, \tag{45}$$

---

[22] For more details see e.g. the review [8].

where the homogeneous equation $\mathcal{L}F_r(W) = 0$ is the same for all F_r, and $g_r(W)$ is the inhomogeneity which does depend on the functions $\{F_s \mid s \leqslant r - 1\}$ and their derivatives. It is easy to check that the function $\Theta(W) = W/(1 + W)$ solves the homogeneous equation $\mathcal{L}\Theta = 0$. This motivates rescaling the F_r to simplify the left-hand-side of (45):

$$F_r(W) = \frac{W}{1 + W} Y_r(W); \qquad \mathcal{L}F_r(W) = W^2 Y_r'(W). \tag{46}$$

The advantage of working with $Y_r(W)$ is that we can give an explicit formula for the solutions:

$$Y_r(W) = \int \mathrm{d}W\, W^{-2} g_r(W) + c_r. \tag{47}$$

The integrand of (47) is found to be given by the recurrence relation:

$$
\begin{aligned}
Y_r'(W) = W^{-2} g_r(W) = {} & \frac{(4 - \beta)(1 + W)}{A W^2} \delta_{1,r} - \frac{8}{A W} Y_{r-1}(W) \\
& + \sum_{k=0}^{r-1} \left[\frac{9 - r}{2A(1 + W)} Y_k(W) Y_{r-k-1}(W) \right. \\
& + \frac{1}{(1 + W)^3} Y_k(W) \left(\frac{\beta}{A} Y_{r-k-1}(W) - (1 - \delta_{k,0}) Y_{r-k}(W) \right) \\
& + \left. \frac{W}{(1 + W)^2} Y_k(W) \left(\frac{\beta}{A} Y_{r-k-1}'(W) - (1 - \delta_{k,0}) Y_{r-k}'(W) \right) \right]. \tag{48}
\end{aligned}
$$

Adding an integration constant c_r in (47) corresponds to adding a multiple of the function $\Theta(W)$, $F_r(W) \to F_r(W) + c_r \Theta(W)$. In general, the rational decomposition of the integrand in (47) includes a term of order W^{-1}, which leads to logarithms in the $Y_r(W)$. There is a unique choice of the set $\{c_r \mid r \geqslant 0\}$ for which the $Y_r(W)$ are rational functions in W without any logarithmic terms. Once the Y_r have been computed, the functions F_r are easily obtained by multiplying the Y_r with the factor $W(1 + W)^{-1}$. Our method allows us to compute as many functions F_r as we want. The first few functions are given by:

$$F_0(W) = 1 + W;$$

$$F_1(W) = \frac{2W^3 + (\beta + 4)W^2 + \beta(\beta + 7)W + \beta}{A(1 + W)};$$

$$
\begin{aligned}
F_2(W) = {} & \frac{1}{2A^2 (1 + W)^3} \Big(4W^6 + (7\beta + 22)W^5 + (8\beta^2 + 70\beta + 32) W^4 \\
& + (\beta^3 + 29\beta^2 + 145\beta + 10) W^3 + (2\beta^3 + 34\beta^2 + 110\beta - 8) W^2 \\
& + (\beta^4 + 11\beta^3 + 34\beta^2 + 10\beta) W + 2 \Big);
\end{aligned}
$$

$$
\begin{aligned}
F_3(W) = {} & \frac{1}{6A^3 (1 + W)^5} \Big(6W^9 + (26\beta + 60) W^8 + (45\beta^2 + 317\beta + 210) W^7 \\
& + (30\beta^3 + 438\beta^2 + 1212\beta + 336) W^6 + (11\beta^4 + 252\beta^3 + 1677\beta^2 + 2050\beta + 254) W^5 \\
& + (44\beta^4 + 708\beta^3 + 3210\beta^2 + 1522\beta + 92) W^4 \\
& + (72\beta^4 + 903\beta^3 + 3054\beta^2 + 297\beta + 42) W^3 \\
& + (-2\beta^6 - 30\beta^5 - 82\beta^4 + 410\beta^3 + 1524\beta^2 - 220\beta + 48) W^2 \\
& + \beta (\beta^5 + 15\beta^4 + 86\beta^3 + 188\beta^2 - 36\beta + 68) W - 18\beta^2 + 12\beta \Big). \tag{49}
\end{aligned}
$$

Note that we have not made a distinction between $F_r(\tau)$ and $F_r(W(\frac{3}{2}\tau))$ to keep our notation simple. In order to obtain the original transasymptotic coefficient functions $F_r(\tau)$ from (26), the variable W in (49) must be replaced by $W(\frac{3}{2}\tau)$.

Appendix D. Coefficients of $\gamma(w)$

We give the first four coefficients of the perturbative expansion of $\gamma(w)$ (see (32)),

$$\gamma(w) = \sum_{n=0}^{\infty} \gamma_n w^{-n}. \tag{50}$$

This expansion solves (31). To simplify the notation, let us define,

$$c \equiv f_{\mathrm{ac}}(w_0) - 1, \tag{51}$$

where $f_{\mathrm{ac}}(w_0)$ is the (numerical) analytical continuation of $f(w)$ from $w = 0$ to $w = w_0$, as explained in section 3. The first four coefficients γ_n are then given by:

$$\gamma_0 = \frac{2}{3} c\, e^c;$$

$$\gamma_1 = -\frac{2e^c}{3A} \left(\beta + 2c^3 + (\beta + 4)c^2 + \beta(\beta + 7)c \right);$$

$$\gamma_2 = \frac{e^c}{3A^2} \Bigg(2\beta \left(\beta^2 + 7\beta - 1 \right) + 4c^5 + 4(\beta + 7)c^4 + \left(5\beta^2 + 41\beta + 38 \right) c^3$$

$$+ 2 \left(\beta^3 + 12\beta^2 + 34\beta + 4 \right) c^2 + \beta \left(\beta^3 + 15\beta^2 + 55\beta + 10 \right) c \Bigg);$$

$$\gamma_3 = -\frac{e^c}{9A^3} \Bigg(3\beta \left(\beta^4 + 15\beta^3 + 51\beta^2 - 18\beta + 4 \right) + 8c^7 + 12(\beta + 10)c^6$$

$$+ 6 \left(3\beta^2 + 33\beta + 83 \right) c^5 + \left(13\beta^3 + 207\beta^2 + 872\beta + 620 \right) c^4$$

$$+ 3 \left(3\beta^4 + 52\beta^3 + 261\beta^2 + 349\beta + 78 \right) c^3$$

$$+ 3 \left(\beta^5 + 21\beta^4 + 142\beta^3 + 321\beta^2 + 74\beta + 16 \right) c^2$$

$$+ \beta \left(\beta^5 + 24\beta^4 + 188\beta^3 + 507\beta^2 + 198\beta + 20 \right) c \Bigg). \tag{52}$$

Appendix E. Lambert-W function

The Lambert-W function (see [52, section 4.13]) is defined as the solution to the equation

$$W(z)\mathrm{e}^{W(z)} = z. \tag{53}$$

The function $W(z)$ has infinitely many branches, which are known as $W_k(z)$, where k is an integer. Only two of those branches, $W_{-1}(z)$ and $W_0(z)$, return real values on subsets of the real line. In the case of our problem, the MIS equation (4), the Lambert-W function appears in the context of the transasymptotic summation (26), where the leading-order contribution in w^{-1} is given by,

$$F_0(\tau(w)) = 1 + W \left(\frac{3}{2} \sigma w^\beta \mathrm{e}^{-Aw} \right). \tag{54}$$

As $w \to +\infty$ we require $f(w) \to 1$. This means that $W(\ldots) \to 0$ in (54). For $k \neq 0$ the branches $W_k(z)$ diverge as $z \to 0$. Therefore, we need to choose the branch W_0 at $w = +\infty$, which admits the Taylor expansion $W_0(z) = z + \ldots$ around $z = 0$ and is hence consistent with the behaviour of $f(w)$ near $w = +\infty$. For large arguments, the branch W_0 admits the following expansion [42]:

$$W_0(z) = L_1 - L_2 + \sum_{k=0}^{\infty} \sum_{m=1}^{\infty} C_{km} L_1^{-(k+m)} L_2^m, \tag{55}$$

where

$$\begin{aligned} L_1 &= \log w; \\ L_2 &= \log(\log w); \\ C_{km} &= \frac{(-1)^{k+m+1}}{m!} \mathrm{Stir}(k+m, k+1). \end{aligned} \tag{56}$$

The expression $\mathrm{Stir}(n,m)$ denotes Stirling circle numbers of the first kind. The presence of logarithmic terms in the expansion 55 explain how logarithmic terms arise in the transseries Ψ in (11) from the transseries $\mathcal{F}$ in (9) when going from $w = +\infty$ to $w = -\infty$. Note that the magnitude of the exponential scale $\tau \sim e^{-Aw}$ changes from small to large when the sign of w is flipped from $(+)$ to $(-)$, which makes it necessary to use the expansion (55). Let us also note that the Lambert-W function has a square root branch point at $z = -e^{-1}$.

Appendix F. Taylor-series method

In the Taylor-series method (see [52, section 3.7(ii)]) we combine, at a regular point $w = w_0$, the Taylor series $f(w) = \sum_{n=0}^{\infty} b_n (w - w_0)^n$ with our differential equation (4) and obtain the recurrence relation:

$$w_0(n+1)b_0 b_{n+1} = A\delta_{n,1} + (Aw_0 + \beta - 4)\delta_{n,0} - \tfrac{1}{2}w_0(n+1)\sum_{m=1}^{n} b_m b_{n+1-m}$$

$$- \tfrac{1}{2}(n+8)\sum_{m=0}^{n} b_m b_{n-m} - Ab_{n-1} - (Aw_0 - 8)b_n, \qquad n \geqslant 0. \tag{57}$$

With this method it is very easy to 'walk' in the complex w-plane. Once we know $b_0 = f(w_0)$ (either from a local expansion at the origin, or a branch-point, or from the asymptotic expansion) we can compute many coefficients in the Taylor-series expansion, and use this Taylor series to make a small step in the complex w-plane, that is, compute $f(w_0 + h)$ and use this as the new b_0.

ORCID iDs

Inês Aniceto https://orcid.org/0000-0002-4468-0066
Daniel Hasenbichler https://orcid.org/0000-0002-5390-5175
Adri Olde Daalhuis https://orcid.org/0000-0001-7525-4935

References

[1] Shen C and Yan L 2020 Recent development of hydrodynamic dodeling in heavy-ion collisions *Nucl. Sci. Tech.* **31** 122

J. Phys. A: Math. Theor. **56** (2023) 195201

I Aniceto *et al*

[2] Gale C, Jeon S and Schenke B 2013 Hydrodynamic modeling of heavy-ion collisions *Int. J. Mod. Phys.* A **28** 1340011

[3] Romatschke P 2010 New developments in relativistic viscous hydrodynamics *Int. J. Mod. Phys.* E **19** 1–53

[4] Heinz U and Snellings R 2013 Collective flow and viscosity in relativistic heavy-ion collisions *Annu. Rev. Nucl. Part. Sci.* **63** 123–51

[5] Heller M P and Spaliński M 2015 Hydrodynamics beyond the gradient expansion: resurgence and resummation *Phys. Rev. Lett.* **115** 072501

[6] Florkowski W, Heller M P and Spalinski M 2018 New theories of relativistic hydrodynamics in the LHC era *Rept. Prog. Phys.* **81** 046001

[7] Bender C M and Orszag S A 1999 *Advanced Mathematical Methods for Scientists and Engineers I: Asymptotic Methods and Perturbation Theory* (New York: Springer Science & Business Media) p 1

[8] Aniceto I, Başar G and Schiappa R 2019 A primer on resurgent transseries and their asymptotics *Phys. Rept.* **809** 1–135

[9] Caliceti E, Meyer-Hermann M, Ribeca P, Surzhykov A and Jentschura U D 2007 From useful algorithms for slowly convergent series to physical predictions based on divergent perturbative expansions *Phys. Rep.* **446** 1–96

[10] Berry M and Howls C 1990 Hyperasymptotics *Proc. R. Soc.* A **430** 653–68

[11] Olde Daalhuis A B and Olver F W J 1995 Hyperasymptotic solutions of second-order linear differential equations. I *Methods Appl. Anal.* **2** 173–97

[12] Costin O 1999 Correlation between pole location and asymptotic behavior for Painlevé I solutions *Commun. Pure Appl. Math.* A **52** 461–78

[13] Costin O 2001 On the formation of singularities of solutions of nonlinear differential systems in antistokes directions *Invent. Math.* **145** 425–85

[14] Costin O, Costin R and Huang M 2015 Tronquée solutions of the Painlevé equation PI *Constr. Approx.* **41** 467–94

[15] Aniceto I, Schiappa R and Vonk M (in preparation)

[16] Behtash A, Kamata S, Martinez M and Shi H 2019 Dynamical systems and nonlinear transient rheology of the far-from-equilibrium bjorken flow *Phys. Rev.* D **99** 116012

[17] Behtash A, Kamata S, Martinez M, Schäfer T and Skokov V 2021 Transasymptotics and hydrodynamization of the Fokker-Planck equation for gluons *Phys. Rev.* D **103** 056010

[18] Bjorken J D 1983 Highly relativistic nucleus-nucleus collisions: the central rapidity region *Phys. Rev.* D **27** 140

[19] Müller I 1967 Zum Paradoxon der Wärmeleitungstheorie *Z. Phys.* **198** 329–44

[20] Israel W and Stewart J M 1979 Transient relativistic thermodynamics and kinetic theory *Ann. Phys., NY* **118** 341–72

[21] Ruggeri T, Liu I S and Müller T 1986 Relativistic thermodynamics of gases *Ann. Phys.* **169** 191

[22] Geroch R and Lindblom L 1991 Causal theories of dissipative relativistic fluids *Ann. Phys.* **207** 394–416

[23] Başar G and Dunne G V 2015 Hydrodynamics, resurgence and transasymptotics *Phys. Rev.* D **92** 125011

[24] Aniceto I and Spaliński M 2016 Resurgence in extended hydrodynamics *Phys. Rev.* D **93** 0000054

[25] Heller M P, Janik R A and Witaszczyk P 2012 The characteristics of thermalization of boost-invariant plasma from holography *Phys. Rev. Lett.* **108** 201602

[26] Bhattacharyya S, Minwalla S, Hubeny V E and Rangamani M 2008 Nonlinear fluid dynamics from gravity *J. High Energy Phys.* JHEP02(2008)045

[27] Baier R, Romatschke P, Son D T, Starinets A O and Stephanov M A 2008 Relativistic viscous hydrodynamics, conformal invariance and holography *J. High Energy Phys.* JHEP04(2008)

[28] Behtash A, Kamata S, Martinez M and Shi H 2019 Dynamical systems and nonlinear transient rheology of the far-from-equilibrium Bjorken flow *Phys. Rev.* D **99** 116012

[29] Berry M V and Howls C J 1991 Hyperasymptotics for integrals with saddles *Proc. R. Soc.* A **434** 657–75

[30] Olde Daalhuis A B 1995 Hyperasymptotic solutions of second-order linear differential equations. II *Methods Appl. Anal.* **2** 198–211

[31] Olde Daalhuis A B 2005 Hyperasymptotics for nonlinear ODEs. I. A Riccati equation *Proc. R. Soc.* A **461** 2503–20

J. Phys. A: Math. Theor. **56** (2023) 195201

I Aniceto *et al*

[32] Olde Daalhuis A B 1998 Hyperasymptotic solutions of higher order linear differential equations with a singularity of rank one *R. Soc. Lond. Proc. Ser. A Math. Phys. Eng. Sci.* **454** 1–29

[33] Olde Daalhuis A B 1998 Hyperterminants. II *Proc. R. Soc.* A **89** 87–95

[34] Delabaere E and Pham F 1999 Resurgent methods in semi-classical asymptotics *(Ann. Inst. Henri Poincare Phys. Theor.)* AIHP **71** 1–94 (available at: www.numdam.org/item?id=AIHPA_1999_ _71_1_1_0)

[35] Aniceto I and Schiappa R 2015 Nonperturbative ambiguities and the reality of resurgent transseries *Commun. Math. Phys.* **335** 183–245

[36] Olde Daalhuis A B 2005 Hyperasymptotics for nonlinear ODEs. II. The first Painlevé equation and a second-order Riccati equation *Proc. R. Soc.* A **461** 3005–21

[37] Aniceto I, Hasenbichler D, Howls C J and Lustri C J 2021 Capturing the cascade: a transseries approach to delayed bifurcations *Nonlinearity* **34** 8248

[38] Aniceto I Talk at StringMath 2019, From asymptotics to exact results in string and gauge theories in Uppsala, Sweden (available at: www.stringmath2019.se/scientific-talks-2/)

[39] Borinsky M and Dunne G V 2020 Non-perturbative completion of Hopf-algebraic Dyson-Schwinger equations *Nucl. Phys.* B **957** 115096

[40] Trefethen L N and Weideman J A C 2014 The exponentially convergent trapezoidal rule *SIAM Rev.* **56** 385–458

[41] Edgar G 2010 Transseries for beginners *Real Anal. Exch.* **35** 253–310

[42] Corless R M, Gonnet G H, Hare D E G, Jeffrey D J and Knuth D E 1996 On the Lambert*W* function *Adv. Comput. Math.* **5** 329–59

[43] Aniceto I Hasenbichler D and Olde Daalhuis A B (in preparation)

[44] Heller M P, Serantes A, Spaliński M, Svensson V and Withers B 2022 Relativistic hydrodynamics: a singulant perspective *Phys. Rev.* X **12** 041010

[45] Heller M P and Svensson V 2018 How does relativistic kinetic theory remember about initial conditions? *Phys. Rev.* D **98** 054016

[46] Behtash A, Kamata S, Martinez M and Shi H 2020 Global flow structure and exact formal transseries of the Gubser flow in kinetic theory *J. High Energy Phys.* JHEP07(2020)226

[47] Aniceto I 2016 The resurgence of the cusp anomalous dimension *J. Phys. A: Math. Theor.* **49** 065403

[48] Dorigoni D and Hatsuda Y 2015 Resurgence of the cusp anomalous dimension *J. High Energy Phys.* JHEP09(2015)138

[49] Romatschke P 2017 Relativistic hydrodynamic attractors with broken symmetries: non-conformal and non-homogeneous *J. High Energy Phys.* JHEP12(2017)079

[50] Du X, Heller M P, Schlichting S and Svensson V 2022 Exponential approach to the hydrodynamic attractor in Yang-Mills kinetic theory *Phys. Rev.* D **106** 014016

[51] Olde Daalhuis A B and Olver F W J 1995 On the calculation of Stokes multipliers for linear differential equations of the second order *Methods Appl. Anal.* **2** 348–67

[52] Olver F W J, Olde Daalhuis A B, Lozier D W, Schneider B I, Boisvert R F, Clark C W, Miller B R, Saunders B V, Cohl H S and McClain M A (eds) 2022 *NIST Digital Library of Mathematical Functions* (available at: http://dlmf.nist.gov/ Release 1.1.5 of 03 March)